

Boston University**OpenBU****<http://open.bu.edu>**

Biology

BU Open Access Articles

2019-11-12

BowSaw: inferring higher-order trait interactions associated with complex biological phenotypes

This work was made openly accessible by BU Faculty. Please [share](#) how this access benefits you. Your story matters.

Version	Accepted manuscript
Citation (published version):	Mark Kon, Demetrius Dimucci, Daniel Segre. 2019. "BowSaw: inferring higher-order trait interactions associated with complex biological phenotypes." BioArXiv, https://doi.org/10.1101/839357

<https://hdl.handle.net/2144/40879>

Boston University

BowSaw: inferring higher-order trait interactions associated with complex biological phenotypes

Demetrius DiMucci^{a,b}, Mark Kon^{a,c}, Daniel Segrè^{a,b,d, #}

^a Bioinformatics Graduate Program, Boston University, Boston, Massachusetts, USA

^b Biological Design Center, Boston University, Boston, Massachusetts, USA

^c Department of Mathematics and Statistics, Boston University, Boston, Massachusetts, USA

^d Department of Biology, Department of Biomedical Engineering, Department of Physics, Boston University, Boston, Massachusetts, USA

Correspondence to Daniel Segrè, dsegre@bu.edu

Abstract

Machine learning is helping the interpretation of biological complexity by enabling the inference and classification of cellular, organismal and ecological phenotypes based on large datasets, e.g. from genomic, transcriptomic and metagenomic analyses. A number of available algorithms can help search these datasets to uncover patterns associated with specific traits, including disease-related attributes. While, in many instances, treating an algorithm as a black box is sufficient, it is interesting to pursue an enhanced understanding of how system variables end up contributing to a specific output, as an avenue towards new mechanistic insight. Here we address this challenge through a suite of algorithms, named BowSaw, which takes advantage of the structure of a trained random forest algorithm to identify combinations of variables (“rules”) frequently used for classification. We first apply BowSaw to a simulated dataset, and show that the algorithm can accurately recover the sets of variables used to generate the phenotypes through complex Boolean rules, even under challenging noise levels. We next apply our method to data from the integrative Human Microbiome Project and find previously unreported high-order combinations of microbial taxa putatively associated with Crohn’s disease. By leveraging the structure of trees within a random forest, BowSaw provides a new way of using decision trees to generate testable biological hypotheses.

23 Introduction

24 The production of large biological data sets with high-throughput techniques has
 25 increased the utilization of supervised machine learning algorithms to produce
 26 predictions of complex phenotypes (e.g. healthy vs. disease) from measurable traits.
 27 These algorithms use measurements of relevant traits such as gene variants, the
 28 presence/absence of microbial taxa, or metabolic consumption variables as predictors.
 29 Categorical prediction of phenotypes is typically the end goal of these applications.
 30 However, an additional benefit of these algorithms is the potential to extract explanatory
 31 classification rules. In this context, a rule is defined as a Boolean function of a set of
 32 traits, such that the value of the function is 1 (true) when the traits are associated with a
 33 given phenotype. Identifying the relationships between the traits involved in
 34 classification rules may yield key insights into the biological processes associated with
 35 important phenotypes [1, 2]. This realization is creating demand for methods that assist in
 36 the interpretation of supervised machine learning methods [3–5], especially when the
 37 measured traits may be causal agents of disease states, such as genetic variants or
 38 microbial taxa [6]. Identifying classification rules associated with a phenotype of interest
 39 is valuable because these rules are likely to carry information about the causal
 40 mechanisms that generate the phenotype.

41 Algorithms that are particularly valuable in this respect are those involving
 42 decision trees, such as random forests, since decision trees are easily interpretable [7].
 43 Decision trees are rule-based classifiers, where rules arise from a series of “yes-no”
 44 questions that can efficiently divide the data into categorical groups. In a biological

context, such rules may arise from sets of genes whose simultaneous modulation could affect a phenotype, or sets of microbial species whose co-occurrence may be associated with a disease state. While in several cases it seems like disease phenotypes are uniquely associated with a single specific pattern (e.g. retinoblastoma [8]), there is increasing evidence for cases in which multiple distinct patterns can be associated with (and potentially causing) the same high-level phenotype [9, 10]. A particular example we will explore in this work is the multiplicity of distinct microbial presence/absence patterns which may be associated with Crohn's disease [11]. Crohn's disease has five clinically defined sub-types [12] but studies of the associated microbiome do not usually indicate which form of Crohn's disease a donor has been diagnosed with. Each sub-type of the disease may be associated with different microbes, each requiring different treatment regimes. Thus, identifying rules associated with sub-populations within a given phenotype label are of great interest due to potential therapeutic implications.

The fact that there may be multiple etiologies that generate the same or similar phenotypes complicates the straightforward interpretation of parameter coefficients or variable importance scores [13, 14]. Uncovering the multiple interactions between predictive variables as they relate to phenotypic labels remains a challenging statistical endeavor, but one that is of paramount importance. Identifying the associated rules that a random forest uses to classify a given sample as having a particular disease enables the development of mechanistic hypotheses for follow up-studies. This challenge, and an overview of the key strategy we propose, are illustrated in Figure 1. In figure 1A we depict a toy model where measured variables (traits) have only two possible values (e.g.:

67 present/absent), the high-level phenotype (category) is binary (e.g.: no disease/disease),
 68 and two distinct Boolean rules can both generate the phenotype. The goal in this case is
 69 to identify each of the rules that are associated with the phenotype. The multiple Boolean
 70 rules obtained in this manner can be thought of as a consensus decision tree that
 71 possesses the most informative branches of the forest with respect to a given class label.
 72 In this work, we will show how this can be achieved by in-depth analyses of any given
 73 random forest (RF) (Fig. 1B).

74 The random forest algorithm intrinsically takes advantage of non-linear
 75 relationships between variables and is widely used in the life sciences [15–17]. RFs,
 76 when used to distinguish between disease states known to have multiple causes, often
 77 result in excellent classifiers [18, 19]. It has also been reported that RFs capture subtle
 78 statistical interactions between variables [13]. Unfortunately, an RF is not
 79 straightforwardly interpretable despite its hierarchical structure, and recovering those
 80 interactions is notoriously difficult [14] due in large part to the method’s reliance on
 81 ensembles of trees [20]. The difficulties in interpretation created by these properties has
 82 led many to refer to RF as a ‘black box’ model [21].

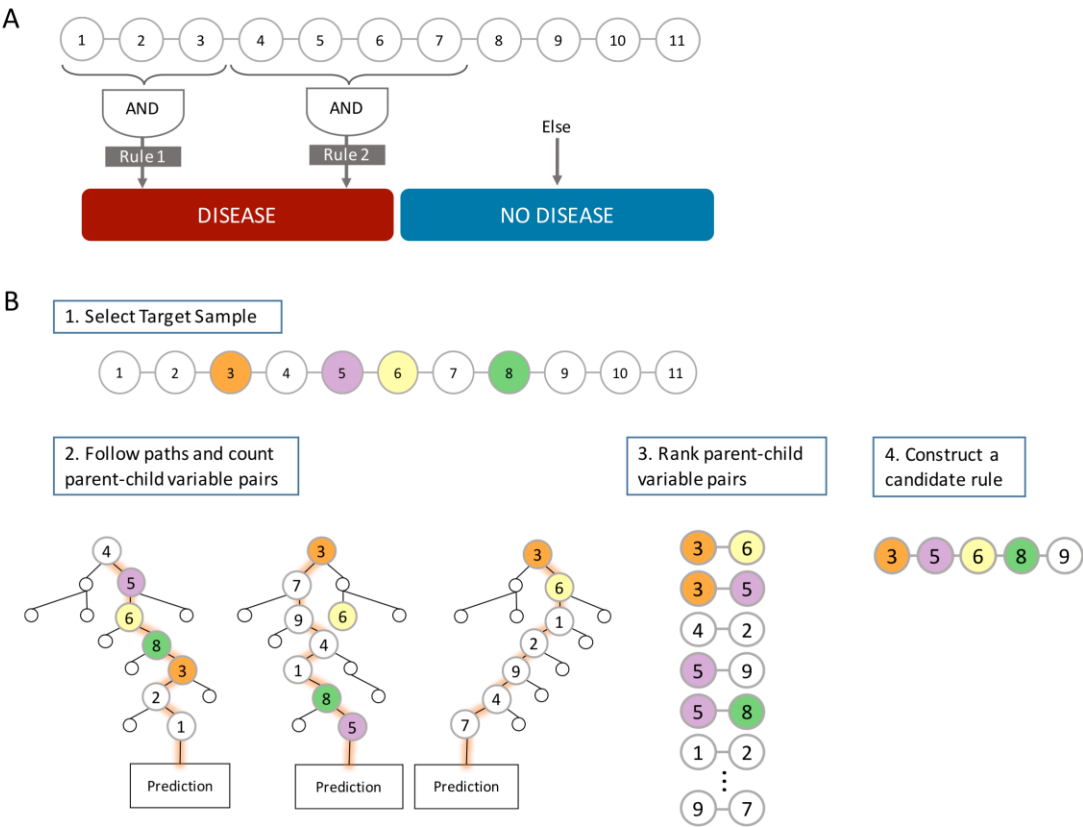
83 Identifying the rules that a RF utilizes in classification tasks is an active area of
 84 research, and many strategies have been developed to address this problem. Effective
 85 strategies have focused on evaluating how individual variables influence the
 86 classification probabilities of specific samples [22, 23], pruning existing decision rules
 87 found in the tree ensemble to produce compact models [24], computing conditional
 88 importance scores [25], or iteratively enriching the most prevalent variable co-

occurrences through regularization [26]. These approaches offer valuable methods for the identification of statistical interactions between variables. However, we and others have observed that while these methods are capable of recovering a true causal rule in simulated data when exactly one such rule is present, the existence of multiple rules associated with one phenotype can confound interpretation efforts [26].

Here we describe BowSaw, a new set of algorithms that utilizes variable interactions in a trained RF model in order to extract multiple candidate explanatory rules. With BowSaw, we set out to develop a *post hoc* method intended to aid in the discovery of these rules when the input variables are categorical in nature. The primary approach of BowSaw is to start by approximating a best combination of variables (i.e. a rule) that explain the forest's predictions for individual instances of a given class in the data set and then to curate the collection of best combinations to obtain a concise set of combinations that collectively segregate a class of interest with high precision. For individual instances a rule is identified by systematically quantifying the co-occurrence of specific variable pairs across trees in the forest that attempt to predict the class of the instance (out-of-bag trees) and then using the frequency of co-occurring variable pairs to guide the construction of a rule that precisely identifies the instance as its observed class. For the entire set of instances, we then curate the collection of all rules identified this way in order to produce a small set of rules that are broadly and precisely applicable to instances of the given class label.

We first demonstrate that BowSaw can recover true rules by applying the algorithms to simulated data sets of varying complexity. We then apply BowSaw to a

111 study on the role of the gut microbiome on Crohn’s disease [11], and show that it can find
112 a previously unreported combination of microbial taxa that is broadly and precisely
113 associated with Crohn’s disease instances in the data set. In its current implementation
114 BowSaw can be applied to any dataset with categorical or discrete predictors with any
115 number of class labels.



116 **A** In a hypothetical dataset there may be two phenotype labels – “Disease” and “No
117 Disease”, that we wish to discriminate based on input predictor variables. In this
118 example, there are two distinct high-order patterns that both confer the “Disease”
119 phenotype. Our goal is to identify a potentially diverse set of patterns (or, in this
120 simplified case, all patterns) that are associated with the “Disease” label. **B** Conceptual
121 pipeline of BowSaw. In (1) we begin by identifying the vector of a target instance that
122 has the target observed label. In this example, the colored nodes indicate a true associated
123 pattern, which is unknown to us. In (2) we follow the path of the instance through each of
124 its out-of-bag trees and record how often the sample encounters sequential pairs of
125 variables. (3) Each ordered pair sequence is sorted in descending order by its observed
126

frequency. (4) Starting from the top of the list, pair sequences are iteratively evaluated and added to an undirected network of variables (i.e. a candidate rule) until this network is maximally associated with the observed phenotype of the target vector or the list of ordered pairs is exhausted. Each sample with the label of interest yields one such candidate rule. These rules are then aggregated and curated to obtain a concise set of rules that explain class-specific classification decisions that occur in the forest.

Methods

Overview of the pipeline

Provided with a trained random forest and a training set, BowSaw goes through three steps in order to generate a candidate rule (variable-value combination) for each observation associated with the phenotype of interest. First, for a specific observation, the *Count* algorithm counts the frequency of unique ordered pairs of variables encountered along each of its out-of-bag trees in the forest (Figure 1B – step 2). Second, for that observation, the *Construct* algorithm takes the counts from the first step and generates a list of ordered pairs, ranked by their frequencies, then uses this list as a guide to construct a candidate decision rule (which could consist of two or more variables) that is maximally associated with the observed phenotype (Figure 1B – steps 3 - 4). Finally, the *Curate* algorithm pools the candidate decision rules from each observation together in order to select a subset of rules that collectively account for all of the samples with the desired phenotype (Figure 1B – step 5). Optionally, the *Sub-rule* algorithm can be used to generate pruned versions of candidate rules prior to applying the Curate algorithm in order to obtain a more concise, albeit less specific, set of candidate rules. The Count and Curate algorithms generate the candidate rules for individual observations while the

Curate and Sub-rule algorithms produce a combined set of rules that account for all observations with the chosen phenotype.

In the following section, we provide a description of the inputs BowSaw takes and the algorithms that implement these steps along with pseudocode.

Inputs

BowSaw takes as inputs a dataset, \mathbf{D} , composed of N observed vectors \mathbf{x}_i (together with their respective classes k_i) each of p categorical variables. There are assumed to be K possible class labels for each vector in \mathbf{D} which for the purposes of this discussion denote different phenotypes. A random forest is assumed to be trained on \mathbf{D} to distinguish the classes $k = 1, \dots, K$. Additionally, BowSaw takes as input the feature vector \mathbf{x}_i of a specific observation for which the goal is to identify a set of simplified rules associated with the phenotype k_i .

Counting stubs

Given an RF machine \mathbf{M} trained on dataset \mathbf{D} and a feature vector $\mathbf{x} = (x_1, x_2, \dots, x_p) \in \mathbf{D}$, the first sub-routine of our method (the *count algorithm*) proceeds as follows. It starts by identifying among the set of trees in \mathbf{M} , those sub-paths (sequences of successive variable indices) encountered by sample \mathbf{x} as it travels through \mathbf{M}_x , its set of out-of-bag trees. An out-of-bag tree is a tree for which \mathbf{x} was not included in the training set. For a specific path \mathbf{P} in \mathbf{M}_x the sequence of successive variable indices forms a vector $\mathbf{v} = (v_1, \dots, v_r)$ (note that each v_j is one of the variables x_j). Each stub (ordered pair of

173 sequentially encountered variables $v_i v_{i+1}$) in all out-of-bag along \mathbf{P} for $i = 1, \dots, r-1$ is
 174 accounted for in a $p \times p$ matrix \mathbf{C}^x , where the element C_{ij}^x records the number of stubs
 175 containing the ordered pair of variables x_i and x_j among all paths of \mathbf{M}_x .

176

177 **Algorithm 1: Count Algorithm Pseudocode**

178 Initialize \mathbf{C}^x as a $p \times p$ matrix of zeros.

179 For each path \mathbf{P} with feature indices \mathbf{v} in \mathbf{M}_x do:

180 For $i = 1, \dots, r - 1$,

181 $C_{v_i, v_{i+1}}^x = C_{v_i, v_{i+1}}^x + 1$

182 End loop

183 End loop

184 Return \mathbf{C}^x .

185 For simplicity, henceforth we will denote $\mathbf{C} = \mathbf{C}^x$, remembering that \mathbf{C} continues to
 186 depend on the fixed sample \mathbf{x} .

187

188 **Constructing a candidate rule**

189 A rule for classifying to a test point \mathbf{x} will have the form “ $\mathbf{x}_I = \mathbf{a}_I$ implies \mathbf{x} is in class

190 k ”. Here I is a designated subcollection of the variable indices $i = 1, \dots, p$, and $\mathbf{x}_I =$

191 $(x_{i_1}, \dots, x_{i_{|I|}})$ is the sub-vector of current vector $\mathbf{x} = (x_1, \dots, x_p)$ corresponding just to the

192 indices $i_j \in I$. The vector $\mathbf{a}_I = (a_{i_1}, \dots, a_{i_{|I|}})$ will denote an assigned set of values to the

193 x_i , i.e., so that $x_i = a_i$ for $i \in I$. Thus the condition $\mathbf{x}_I = \mathbf{a}_I$ means assignment of values

194 to x_i for $i \in I$. The rule is that if training vector \mathbf{x} satisfies $\mathbf{x}_I = \mathbf{a}_I$, we classify \mathbf{x} into
195 category k .

196

197 The second sub-routine (the *construct algorithm*) builds a candidate rule \mathbf{R} , based
198 (initially) on a fixed training point, say $\mathbf{a} \in \mathbf{D}$, in class k . This is done by first placing all
199 of the stubs (i, j) with non-zero counts \mathbf{C}_{ij} into a list \mathbf{L} sorted in descending order by their
200 values in \mathbf{C} .

201

202 We define the candidate rule \mathbf{R} (based on \mathbf{a}) through the following steps. We initialize
203 using the first stub $L_1 = (i_1, j_1)$ in the list \mathbf{L} , together with the two fixed values $x_{i_1} =$
204 a_{i_1} , $x_{j_1} = a_{j_1}$. This is the initialized form of the rule \mathbf{R} , which requires that for any test
205 vector, its values at the above indices i_1 and j_1 match the values

206 of the above fixed training vector $\mathbf{a} \in \mathbf{D}$, so that $x_{i_1} = a_{i_1}$, and $x_{j_1} = a_{j_1}$. For brevity,
207 denote the pair $(i_1, j_1) = I_1$ and the corresponding assigned values as $(a_{i_1}, a_{j_1}) = \mathbf{a}_{I_1}$.

208 Then the content of rule \mathbf{R} will be denoted succinctly as $\mathbf{R}: \mathbf{x}_I = \mathbf{a}_I \Rightarrow \text{class } k$. Since
209 ordering of the indices i_1, j_1 does not matter, (as long as the indices are identified), we
210 will henceforth write $(i_1, i_2) \rightarrow \{i_1, i_2\}$.

211 We then update rule \mathbf{R} as follows. We find all $\mathbf{x} \in \mathbf{D}$ that satisfy the initial part of rule \mathbf{R} ,
212 i.e., $\mathbf{x}_I = \mathbf{a}_I$ i.e., all training points matching the two indices $\{i_1, j_1\}$ of training sample \mathbf{a} ,
213 and store them as a subcollection $\mathbf{D}_1 \subset \mathbf{D}$ of the training set. We call F the fraction of
214 data points in \mathbf{D}_1 that have phenotype k , i.e., match the phenotype of the initial sample
215 $\mathbf{a} \in \mathbf{D}$. If $F = 1$, we stop and return the current above rule \mathbf{R} . If $F < 1$, we continue by

216 choosing the second stub $L_2 = \{i_2, j_2\}$ in the above list L , and augment the current rule R
 217 by adding the condition $x_{i_2} = a_{i_2}, x_{j_2} = a_{j_2}$ (again written $x_{I_2} = \mathbf{a}_{I_2}$) and maintaining the
 218 assignment of class k (i.e., the same class as the currently fixed sample $\mathbf{a} \in D$). If the
 219 second stub L_2 happens to overlap with the initial stub L_1 , this added condition in the rule
 220 R will clearly be consistent, being still based on the fixed sample \mathbf{a} . We augment the
 221 current index list I_1 to a list I_2 , adding to it the two new indices i_2 and j_2 , so that now
 222 $I_2 = \{i_1, j_1, i_2, j_2\}$ writing the augmented rule as $R: x_{I_2} = \mathbf{a}_{I_2} \Rightarrow \text{class } k$. Again
 223 defining F to be the fraction of the data subset D_2 (matching the more restrictive new
 224 rule R) with phenotype k , we stop the algorithm and use the current rule R if $F = 1$, and
 225 otherwise augment rule R by adding the indices $L_3 = (i_3, j_3)$ to it, as above, yielding a
 226 larger set I_3 of indices and the augmented rule $R: x_{I_3} = \mathbf{a}_{I_3} \Rightarrow \text{class } k$, with a more
 227 restricted subset $D_3 \subset D$, and a new value for F , now the fraction of D_3 in the class k of
 228 the fixed $\mathbf{a} \in D$.
 229 This process continues until the fraction $F = 1$, i.e., 100% of the samples in D match the
 230 current set of indices, and also match the class k of the current sample \mathbf{a} . Alternatively,
 231 the algorithm stops when all stubs in L have been exhausted.

232

233 **Algorithm 2: Construct Algorithm Pseudocode**

234 Make ranked list L of stubs from C

235 Initialize fixed $\mathbf{a} \in D$, $R = \phi$, $I = \phi$, $F = 0$,

236 For $i = 1: |L|$, select stub L_i

237 If $F = 1$:

238 Exit loop

239 Else:

240 $I' = \{I \cup L_i\}$

241 $D_{I'} = \{x \in D: x_{I'} = a_{I'}\}$

242 $F' = \frac{|\{x \in D_{I'}: \text{class } x=k\}|}{|D_{I'}|}$

243 If $F' > F$:

244 $I = I'$

245 $F = F'$

246 End loop

247 Return I, F, D_I [all corresponding to the fixed $a \in D$].

248 Return rule $R: x_I = a_I \Rightarrow \text{class } k$

249

250 Curating candidate rules:

251 The *count* and *construct* algorithms are the heart of BowSaw. In our workflow,

252 we apply these algorithms to each observation $a \in D$ that has the desired observed

253 phenotype k . We call the set of these vectors $D^k \subset D$. By default, we produce a single

254 candidate rule for each vector in $a \in D^k$. We store each candidate rule in list Q and rank

255 them by their respective values of $|I|$, i.e., the number of indices in the respective rules.

256 Since Q may include many redundant rules, we developed another sub-routine (the *curate*

257 *algorithm*) to generate a concise set of candidate rules that collectively account for all

258 data vectors D^k in class k . Briefly, we initialize an empty list E , to which we add the top

259 ranked rule from \mathbf{Q} (by default this is the rule with the greatest value of $|\mathbf{I}|$), and record
 260 the index of samples in \mathbf{D} that match any rule in \mathbf{E} and also have the desired observed
 261 phenotype class k , into a set \mathbf{A} . Next, we determine how many samples remain
 262 unaccounted for, i.e. are in $\mathbf{U} = \mathbf{D}^k \sim \mathbf{A}$, Then we determine which of the remaining rules
 263 in \mathbf{Q} minimizes $|\mathbf{U}|$, add it to \mathbf{E} , and repeat these steps until \mathbf{U} is an empty set.

264

265 Algorithm 3: Curate algorithm pseudocode

266 \mathbf{Q} = ranked list of all candidate rules for Φ_t

267 $\mathbf{E} = \mathbf{Q}_{best}$ (user defined, default is maximum \mathbf{M})

268 \mathbf{I}^* = which \mathbf{D} match any rule in \mathbf{E} and $k = \mathbf{K}_d$

269 $\mathbf{A} = \mathbf{D}^k \cap \mathbf{M}^*$

270 $\mathbf{U} = \mathbf{D}^k - \mathbf{A}$

271 While \mathbf{U} is not empty:

272 $\mathbf{B} = \{ \}$

273 For rule i in \mathbf{Q} :

274 $\mathbf{E}^* = \mathbf{E} + \mathbf{Q}_i$

275 \mathbf{I}^* = which \mathbf{D} match any rule in \mathbf{E}^* and $k = \mathbf{K}_d$

276 $\mathbf{A}^* = \mathbf{D}^k \cap \mathbf{I}^*$

277 $\mathbf{B}_i = |\mathbf{U} - \mathbf{A}^*|$

278 End loop

279 $best = \text{which min } \mathbf{B}_i$

280 $\mathbf{E} = \mathbf{E} + \mathbf{Q}_{best}$

281 $M^* = \text{which } D \text{ match any rule in } E \text{ and } k = K_d$

282 $A = D^k \cap M^*$

283 $U = U - A$

284 End while loop

285 Return E

286

287 Constructing sub-rules

288 Since rules are rarely 100% associated with any given phenotype, we devised a
 289 strategy for selecting a set of candidate sub-rules that account for all samples with desired
 290 observed phenotype class k . Candidate sub-rules are shorter candidate rules derived from
 291 larger candidate rules by omitting one or more variables. For each candidate rule in E , we
 292 identify sub-rules that meet a user-defined complexity criteria, e.g. only produce sub-
 293 rules that are composed of three or four variables and their corresponding values. We
 294 place each of the unique sub-rules into a new list E_{sub} . Then the corresponding number of
 295 identical matches, I , and proportion of I that have the phenotype K_d , F , are determined.
 296 At this stage, we can apply our third sub-routine (the *Curate* algorithm) to E_{sub} to obtain a
 297 parsimonious list of sub-rules that accounts for \mathbf{x}_{all} . In our pipeline, we also choose
 298 thresholds based on desired levels of I and/or F in order to eliminate poor candidate sub-
 299 rules from consideration. In this study, we decided on the thresholds after visually
 300 inspecting a plot of F against I .

301

302 Algorithm 4: Sub-rule algorithm pseudocode

303 $E_{sub} = \{ \}$

304 $Complexity = \{ \text{user defined numeric values} \}$

305 For $rule$ in E

306 For i in $Complexity$

307 $E_{sub} = E_{sub} \cup (\frac{rule}{i})$

308 End loop

309 End loop

310

311 The algorithms described above are generalizable to multi-classification tasks but
312 are currently limited to discretized or categorical representations of the feature space.

313 Pseudocode for implementing each of the algorithms described above along with an
314 implementation of the algorithms in R [27] can be found in the supplemental files and on
315 github: <https://github.com/ddimucci/BowSaw>.

316

317

318 **Results**

319 **Application to simulated Data**

320 To test the capacity of BowSaw to recover multiple decision rules, we applied it
321 to increasingly challenging simulated data sets. These data set consists of binary vectors
322 representing different observations. The phenotype associated with each observation is a
323 function of the corresponding vector. The function consists of a set of multiple mutually
324 distinct Boolean rules, such that if a rule is satisfied, it will cause the observation to have

the phenotype with a certain probability (which we call here “penetrance” because of its resemblance to the genetics concept). The first dataset (IDEALIZED) we use is relatively simple, and includes multiple equally prevalent rules. It is also generated under the assumption that there are no unmeasured confounders, i.e. that if an observation does have a phenotype, then it must be satisfying at least one of the above rules. We then apply BowSaw to a more challenging scenario (INTERMEDIATE) in which the phenotype-generating rules differ in their relative prevalence and the assumption of unmeasured confounders is violated. Finally, is a set of data sets with complex co-varying parameters (COMPLEX), we systematically varied the underlying parameters of the simulation and examined the relationship between summary statistics of the RF performance and the ability of BowSaw to generate candidate rules containing the true phenotype-generating rules.

For the IDEALIZED scenario, we simulated data set of 100 independent and identically distributed random binary variables and 2,000 observations. We randomly defined five rules that each required four randomly selected variables each to have specific values (e.g. all variables equal to 1) in order to assign a hypothetical phenotype with likelihood between .8 and .9. Here we present the results of this scenario with a specified random seed, but other seeds and parameters can be explored using the scripts provided in the supplemental files. Using these parameters 479 samples were assigned the phenotype and BowSaw produced a set of 135 unique candidate rules ranging in complexity from six to fourteen variables. From these rules, we produced all sub-rules ranging involving anywhere from two to five variables, which resulted in unique 50,034

347 sub-rules. We calculated the number of matches $|I|$, the proportion of samples with the
348 phenotype, F , for each sub-rule, and visualized these values in order to select an
349 association threshold (Figure 2A). To reduce the number of sub-rules that the curate
350 algorithm would need to examine, we eliminated from consideration any rules that had an
351 F below 80%. We selected an 80% threshold because in the cluster centered around 125
352 matching samples there is a small cloud of rules that are clearly segregating the
353 phenotype more efficiently than the others are. We selected the sub-rule with largest $|I|$
354 among these as the top candidate rule. This produced a final list consisting of five
355 candidate rules that accounted for all of the samples with the phenotype and were each
356 one of the true phenotype generating rules (Figure 3A red points). These results
357 demonstrate that in an ideal scenario with no phenotype diagnosis errors, BowSaw is
358 indeed capable of recovering multiple true rules.

359 For the more challenging scenario (INTERMEDIATE), we generated the data set
360 the same as before except this time we allowed the five underlying rules to vary in
361 complexity from three to five variables. Varying the complexities of rules resulted in
362 different prevalence among them, as rules that are more complicated are less likely to
363 appear in the data. In this case, we had one rule of complexity five, two that required four
364 variables, and two that used three variables. We also added background noise by
365 randomly assigning the phenotype to 2% of samples that did not possess any of the rules.
366 BowSaw produced 176 unique candidate rules involving between six to thirteen
367 variables. From this list we generated 68,938 sub-rules and chose an association threshold
368 of 75% because there are two clusters at $\sim |I| = 125$ that begin to clearly separate in that

369 range and the two outlier points at $\sim |I| = 250$ do not combine to account for all of the
 370 phenotype (Figure 3B). Applying the curate algorithm to the rules meeting this threshold
 371 produced 20 candidate sub-rules the top four (when ranked by $|I|$) of which were true
 372 rules. The rule of five variables was not recovered. These results show that BowSaw is
 373 able to recover strongly associated patterns (and in this case, causal patterns) even in the
 374 presence of noise, but low prevalence rules can be masked by high prevalence rules.

375 We used the same data generation method to investigate BowSaw's ability to
 376 produce candidate rules containing true rules when the underlying parameters change.
 377 We applied BowSaw to 20,000 simulated data sets where we randomly altered the
 378 number of features, sample size (200 or 2,000 samples), complexity of the rules, number
 379 of rules, the likelihood of each rule assigning the phenotype, and the background noise.
 380 We identified scenarios where rule recovery with BowSaw performs very well and
 381 situations in which it fails to recover any rules at all. Additionally, we found a strong
 382 linear relationship between BowSaw's performance measured as the average fraction of
 383 rules recovered and the of number of samples, number of features, and two evaluation
 384 metrics for RF model – the area under the curve for both the receiver operator
 385 characteristic and precision recall curves (Figure S1).

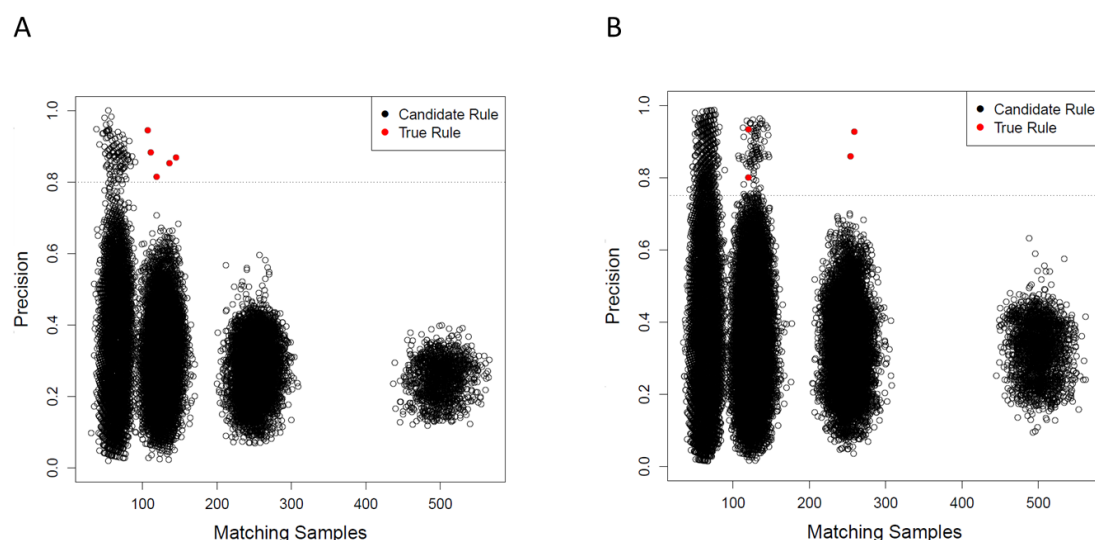


Figure 2

A Precision of candidate sub-rules against the number of exactly matching samples for the ideal scenario. Each point represents a unique sub-rule. X-axis is the number of samples that exactly match the pattern defined by the rule. Y-axis is the fraction of matching samples with the observed phenotype (i.e. precision of the rule). Each cluster of points corresponds to decreasing rule complexity from 5 variables per rule to 2 on the right most cluster. These clusters appear because the values of each variable is produced by an identical binomial distribution. Dashed line is the precision threshold we set. Only candidate rules with precision above this threshold were considered for the curate algorithm. Red points are the causative sub-rules we defined. BowSaw correctly identified all five red points in this scenario. **B** Candidate sub-rules generated for the more challenging scenario. We defined 5 causative rules of varying lengths in this scenario and allowed 2% of samples without a causative rule to be assigned the label. BowSaw completely 4 of the causative rules (red points). The longest rule which involved 5 variables was not recovered.

Application to Human Microbiome Data

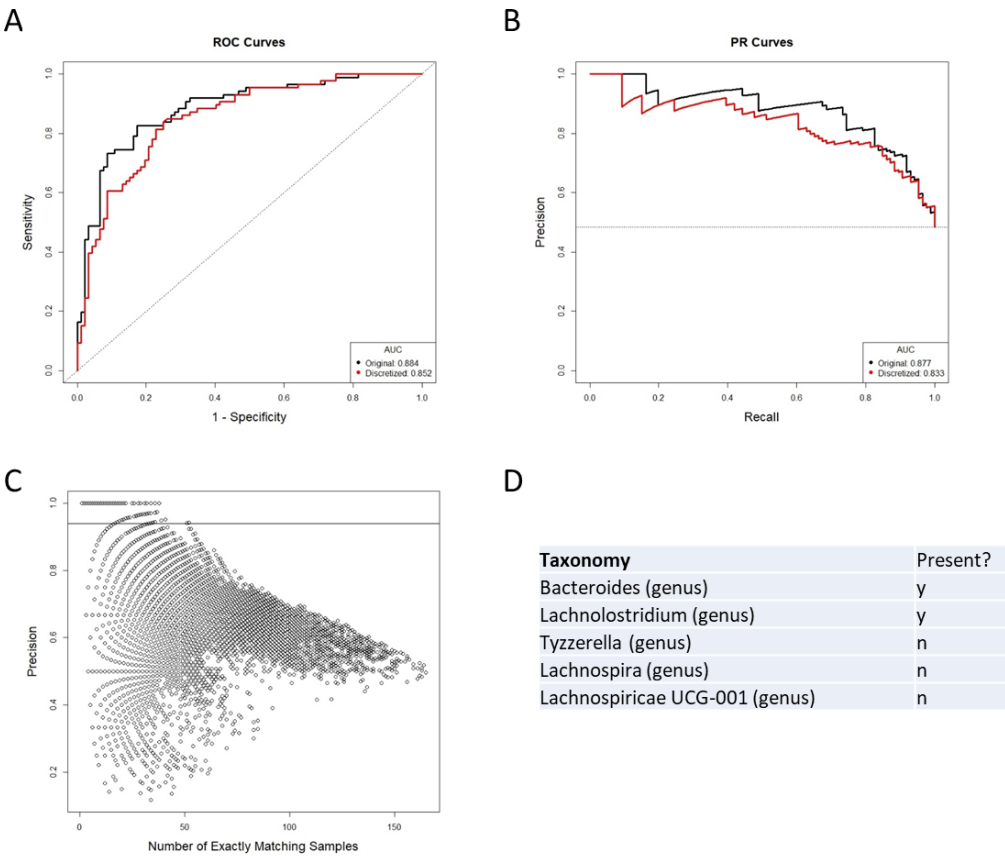
Irregular distributions of microbial taxa within the gut are often associated with serious illnesses such as Crohn's disease or ulcerative colitis [28, 29]. Human microbiome studies regularly use 16s sequencing methods and extensive reference databases to report on microbial taxa found in samples as operational taxon units (OTUs). RF classifiers are frequently built using counts of OTUs to accurately discriminate

409 between disease and healthy patient samples [30, 31]. Despite their demonstrated
 410 effectiveness as good classifiers of Crohn's disease, studies that look to discover
 411 associations with disease status typically focus on individual OTUs while specific
 412 microbial association rules found by RF are not discussed, as a result it is uncertain how
 413 heterogeneous study cohorts are. To investigate potential rule heterogeneity in a human
 414 microbiome cohort we downloaded processed files from the Human Microbiome Project
 415 for inflammatory bowel disease (IBD) [11] which contain information on the taxonomic
 416 profiles of 982 OTUs in 178 patients – 86 of which have been diagnosed with Crohn's
 417 disease, 46 diagnosed with ulcerative colitis, and 46 diagnosed as non-IBD. We were
 418 specifically interested in finding rules that separate the Crohn's disease samples from
 419 ulcerative colitis and non-IBD, so we framed the problem as a binary classification task
 420 with Crohn's disease as the target phenotype.

421 Since the current implementation of BowSaw is limited to finding rules when the
 422 variables have categorical values, we first converted the OTU counts of each taxon to a
 423 simple presence/absence scheme. This resulted in nearly equivalent RF performance
 424 relative to training RF with the original continuous OTU inputs: ROC AUC of 0.862
 425 (binary) vs 0.882 (continuous) and PR AUC of 0.846 (binary) vs 0.886 (continuous)
 426 (Figure 3A-B). This is an important result because it allows us to think about associations
 427 just in terms of presence or absence of an OTU without sacrificing much in model
 428 performance. We applied BowSaw to the Crohn's disease samples and visualized 56,902
 429 resultant sub-rules ranging in complexity from 2 to 7 variables (Figure 3C). There were
 430 1,941 sub-rules with $F = 1$. We selected the most general of these rules ($\max|I|$) to be the

431 top candidate for the curate algorithm and found that it considers the status of 5 OTUs
432 and accounts for 38 of 86 Crohn's disease samples (Figure 3C). We set an association
433 threshold of 90% and ended up with 10 sub-rules that together account for all 86 Crohn's
434 disease samples and an additional 11 non-Crohn's disease samples (4 non-IBD, 7
435 ulcerative colitis). The top five rules combine to account for 78 of 86 Crohn's disease
436 samples and include 10 non-Crohn's disease samples (Table 1).

437 The top candidate rule is comprised of the presence of *Bacteroides* and
438 *Lachnoclostridium* and the absence of three genera from the family *Lachnospiraceae*:
439 *Lachnospira*, *Tyzerrella*, and *Lachnospiraceae* UCG 001 (Figure 3D). Detection of
440 *Bacteroides* was nearly ubiquitous within the cohort, it was found in 170 of 178 total
441 samples, but only 3 of the samples in which it was missing are diagnosed as Crohn's
442 disease. For the remaining taxa we performed a t-test comparing the distribution of the
443 taxa in Crohn's disease versus ulcerative colitis and versus healthy samples.
444 *Lachnoclostridium* was frequently found in Crohn's disease (67/86) but not in ulcerative
445 colitis (27/46, $p = .02$) and was detected at roughly the same rate in non-IBD samples
446 (34/46, $p = .616$). Detection of *Lachnospira* was depleted in Crohn's disease samples
447 (20/86) relative to ulcerative colitis (20/46, $p = .022$) and to non-IBD samples (31/46, $p =$
448 9.9^{-7}). *Tyzerrella* was also detected at a lower rate in Crohn's disease (63/86) relative to
449 ulcerative colitis (24/46, $p = .019$) and non-IBD (24/46, $p = .019$). *Lachnospiraceae* UCG
450 001 was rarely detected in Crohn's disease (4/86) which is a lower rate than it was
451 detected in ulcerative colitis (9/46, $p = .022$) and in non-IBD samples (19/46, $p = 1.45^{-5}$).



452

453

454

455

456

457

458

459

460

461

462

463

464

465

Figure 3

A Performance of the random forest classifier as measured by area under the receiver operator curve (ROC-AUC) is not strongly perturbed by simplifying OTU representation to a presence/absence scheme versus the original continuous count. Dashed line indicates the performance of a perfectly random classifier. **B** The area under the curve of the precision recall curve is similarly not strongly affected by the new representation scheme. Dashed horizontal line is the random performance line. **C** Each point represents a unique candidate sub-rule. On the x-axis is the number of samples in the data matrix that are subject to that rule. The y-axis represents what fraction of matching samples were diagnosed as Crohn's disease. **D** The taxon identities of the OTUs that make up the most generally applicable of the sub-rules where all matching samples have the Crohn's disease label.

Rule	CD Samples	Non CD Samples	New Samples Covered	Taxonomy	Presence
1	38	0	38	<i>Bacteroides</i> (genus)	y
				<i>Lachnospiraceae</i> (genus)	y
				<i>Tyzzerella</i> (genus)	n
				<i>Lachnospira</i> (genus)	n
				<i>Lachnospiraceae</i> UCG-001 (genus)	n
2	41	4	20	<i>Dialister</i> (genus)	y
				<i>Christensenellaceae</i> R7 group (genus)	n
				<i>Christensenellaceae</i> R7 group (genus)	n
				<i>Collinsella</i> (genus)	n
				<i>Ruminococcaceae</i> (family)	n
				<i>Finegoldia</i> (genus)	n
				<i>Ruminococcus</i> 1 (genus)	n
3	9	1	9	<i>Ruminococcus</i> 1 (genus)	y
				<i>Ruminococcaceae</i> UCG-002 (genus)	n
				<i>Lachnospiraceae</i> (family)	n
4	24	2	6	<i>Streptococcus</i> (genus)	y
				<i>Tyzzerella</i> (genus)	n
				<i>Lachnospiraceae</i> (family)	n
				<i>Hafnia</i> <i>Obesumbacterium</i>	n
5	27	3	5	<i>Lachnospiraceae</i> UCG-008 (family)	y
				<i>Ruminococcus</i> 1 (genus)	n
				<i>Eubacterium eligens</i> group	n
6	5	0	2	<i>Ruminococcus</i> 1 (genus)	y
				<i>Dorea</i> (genus)	n
7	7	0	2	<i>Bacteroides</i> (genus)	y
				<i>Dialister</i> (genus)	n
				<i>Eubacterium rectale</i> group	n
8	15	0	2	<i>Lachnospiraceae</i> NK4A136 group	y
				<i>Eubacterium eligens</i> group	y
				<i>Tyzzerella</i> (genus)	n
				<i>Christensenellaceae</i> R7 group (genus)	n
				<i>Lachnospira</i> (genus)	n
9	3	0	1	<i>Ruminococcus gnavus</i> group	y
				<i>Veillonella</i> (genus)	n
				<i>Bacteroides</i> (genus)	n
				<i>Finegoldia</i> (genus)	n
10	10	1	1	<i>Parabacteroides</i> (genus)	y
				<i>Eubacterium eligens</i> group	y
				<i>Ruminococcaceae</i> UCG-003 (genus)	n
				<i>Lachnospiraceae</i> ND3007 group	n

Table 1 Association rules identified by BowSaw that account for all Crohn's disease samples.

Discussion

474 Interpretation of random forest models for classification may be confounded when
475 there are multiple rules (combinations of variables and their specific values) associated
476 with a phenotype of interest. We have developed BowSaw, which is an algorithmic
477 approach for identifying the rules that a trained random forest model uses to make
478 classifications when the values are categorical in nature. By taking advantage of the
479 structure of trees found within a random forest, BowSaw produces a set of multiple
480 decision rules that combine to account for each sample with a given observed phenotype.
481 When the variables are the presumed causal agents, these rules represent plausible
482 mechanistic relationships.

483 Results on simulated data demonstrate that when there are multiple rules
484 associated with a single phenotype label that BowSaw is capable of faithfully identifying
485 them. Application to data from the human microbiome project offers further evidence
486 that BowSaw provides an efficient way of generating plausible hypotheses for high
487 through put metagenomics studies. In particular we identified a rule that utilizes a
488 presence/absence pattern of five microbial taxa (present: *bacteroides*, *lachnoclostridium*,
489 absent: *lachnospira*, *lachnospiracea*, *tyzerrella*) that accounts for nearly half of all
490 Crohn's disease samples in the cohort (38/86). This specific pattern of microbial
491 colonization in the guts of Crohn's disease patients is unreported, but each taxon's
492 respective enrichment or depletion status and association with disease status has been
493 reported. If the cohort of patients in the human microbiome study are representative of all
494 people afflicted by Crohn's disease then this rule represents a significantly large sub-set
495 of those suffering. Inquiries into the relationship of the taxa included in this rule with

disease status may yield important insights into the mechanisms of the disease and potential therapeutic strategies for this sub-population. Of the five associated taxa, we suspect that the absence of *lachnospira*, *lachnospiraceae* UCG 001, and *tyzzerella* are biologically meaningful. We have reason to believe so because it has been reported that the *lachnospiraceae* family is generally suppressed in Crohn's disease [32–34]. *Lachnospira* has been reported as depleted with respect to Crohn's disease several times [35, 36]. The depletion of *tyzzerella* has been associated with chronic intestinal inflammation and supplementation suggested as a probiotic for Crohn's disease [37, 38]. While the relationship of *lachnospiraceae* UCG 001 with Crohn's disease is still unclear, its depletion has been reported in mice displaying symptoms of anhedonia and it was significantly enriched in anhedonia resilient mice [39]. Partly because IBD is frequently accompanied by depression, anhedonia has been suggested as an important symptom in the diagnosis of IBD [40]. The associations of the individual OTUs defined by this rule are consistent with previously reported findings in the existing literature and describe a taxonomic profile that exclusively identifies a large sub-population of Crohn's disease samples within this cohort. The presence of *bacteroides* does not appear to be particularly useful and in this context is probably preserved because it causes a perfect association, although high levels of some species are implicated in the pathology of Crohn's disease [41]. *Lachnoclostridium*, is differentially distributed across the three classes. Notably it is less frequently detected in ulcerative colitis relative to Crohn's and non-IBD samples, which roughly resemble one another. Increased levels of this genus was detected in rats

517 that showed relief of colitis symptoms after treatment with a proposed therapeutic agent
518 [42].

519 The current implementation of the algorithms are restricted to classification tasks
520 with categorical predictor values, this is a challenge that we will need to address in order
521 to make the approach more generally applicable. Future work will also focus on
522 extending these for the interpretation of regression models. Such additions will greatly
523 increase the number of systems to which we can apply BowSaw.

524

525 **Acknowledgments**

526 We are grateful to members of the Segrè lab for helpful discussions and for feedback on
527 the manuscript. DS and DD acknowledge funding from the Defense Advanced Research
528 Projects Agency (Purchase Request No. HR0011515303, Contract No. HR0011-15-C-
529 0091), the U.S. Department of Energy (DE-SC0012627), the NIH (T32GM100842,
530 5R01DE024468, R01GM121950 and Sub_P30DK036836_P&F), the National Science
531 Foundation (1457695), the Human Frontiers Science Program (RGP0020/2016), and the
532 Boston University Interdisciplinary Biomedical Research Office. DD is grateful to Dr.
533 Nisha Rajagopal for her patience in conversations about random forests and her valuable
534 insight.

References

1. Visscher, P. M., Wray, N. R., Zhang, Q., Sklar, P., McCarthy, M. I., Brown, M. A., & Yang, J. (2017). 10 Years of GWAS Discovery: Biology, Function, and Translation. *American Journal of Human Genetics*. doi:10.1016/j.ajhg.2017.06.005
2. Furqan, M. S., & Siyal, M. Y. (2016). Inference of biological networks using Bi-directional Random Forest Granger causality. *SpringerPlus*. doi:10.1186/s40064-016-2156-y
3. Le, V., Quinn, T. P., Tran, T., & Venkatesh, S. (2019). Deep in the Bowel: Highly Interpretable Neural Encoder-Decoder Networks Predict Gut Metabolites from Gut Microbiome. *bioRxiv*. doi:10.1101/686394
4. Azmi, M., Runger, G. C., & Berrado, A. (2019). Interpretable regularized class association rules algorithm for classification in a categorical data space. *Information Sciences*. doi:10.1016/j.ins.2019.01.047
5. Nguyen, M., Wesley Long, S., McDermott, P. F., Olsen, R. J., Olson, R., Stevens, R. L., ... Davisa, J. J. (2019). Using machine learning to predict antimicrobial MICs and associated genomic features for nontyphoidal Salmonella. *Journal of Clinical Microbiology*. doi:10.1128/JCM.01260-18
6. LaPierre, N., Ju, C. J. T., Zhou, G., & Wang, W. (2019). MetaPheno: A critical evaluation of deep learning and machine learning in metagenome-based disease prediction. *Methods*. doi:10.1016/j.ymeth.2019.03.003
7. Brodley, C. E., & Friedl, M. A. (1997). Decision tree classification of land cover

- from remotely sensed data. *Remote Sensing of Environment*. doi:10.1016/S0034-4257(97)00049-7
8. Knudson, A. G. (1971). Mutation and cancer: statistical study of retinoblastoma. *Proceedings of the National Academy of Sciences of the United States of America*. doi:10.1073/pnas.68.4.820
9. Emily, M., Mailund, T., Hein, J., Schauser, L., & Schierup, M. H. (2009). Using biological networks to search for interacting loci in genome-wide association studies. *European Journal of Human Genetics*. doi:10.1038/ejhg.2009.15
10. Leem, S., Jeong, H. H., Lee, J., Wee, K., & Sohn, K. A. (2014). Fast detection of high-order epistatic interactions in genome-wide association studies using information theoretic measure. *Computational Biology and Chemistry*. doi:10.1016/j.compbiolchem.2014.01.005
11. Proctor, L. M., Creasy, H. H., Fettweis, J. M., Lloyd-Price, J., Mahurkar, A., Zhou, W., ... Huttenhower, C. (2019). The Integrative Human Microbiome Project. *Nature*. doi:10.1038/s41586-019-1238-8
12. Reading, D. (2014). Crohn Disease: Pathophysiology, Diagnosis, and Treatment, 85(3), 297–320.
13. Louppe, G. (2014). *Understanding Random Forests*. Cornell University Library.
14. Wright, M. N., Ziegler, A., & König, I. R. (2016). Do little interactions get lost in dark random forests? *BMC bioinformatics*. doi:10.1186/s12859-016-0995-8
15. Boulesteix, A. L., Janitza, S., Kruppa, J., & König, I. R. (2012). Overview of random forest methodology and practical guidance with emphasis on

- computational biology and bioinformatics. *Wiley Interdisciplinary Reviews: Data Mining and Knowledge Discovery*. doi:10.1002/widm.1072
16. Touw, W. G., Bayjanov, J. R., Overmars, L., Backus, L., Boekhorst, J., Wels, M., & Sacha van Hijum, A. F. T. (2013). Data mining in the life science with random forest: A walk in the park or lost in the jungle? *Briefings in Bioinformatics*. doi:10.1093/bib/bbs034
17. Nguyen, C., Wang, Y., & Nguyen, H. N. (2013). Random forest classifier combined with feature selection for breast cancer diagnosis and prognostic. *Journal of Biomedical Science and Engineering*. doi:10.4236/jbise.2013.65070
18. Franzosa, E. A., Sirota-Madi, A., Avila-Pacheco, J., Fornelos, N., Haiser, H. J., Reinker, S., ... Xavier, R. J. (2019). Gut microbiome structure and metabolic activity in inflammatory bowel disease. *Nature Microbiology*. doi:10.1038/s41564-018-0306-4
19. Duvallet, C., Gibbons, S. M., Gurry, T., Irizarry, R. A., & Alm, E. J. (2017). Meta-analysis of gut microbiome studies identifies disease-specific and shared responses. *Nature Communications*. doi:10.1038/s41467-017-01973-8
20. Breiman, L. (2001). Random forests. *Machine Learning*, 45(1), 5–32. doi:10.1023/A:1010933404324
21. Castelvechi, D. (2016). Can we open the black box of AI? *Nature*. doi:10.1038/538020a
22. Welling, S. H., Refsgaard, H. H. F., Brockhoff, P. B., & Clemmensen, L. H. (2016). Forest Floor Visualizations of Random Forests. *arXiv*. Retrieved from

<http://arxiv.org/abs/1605.09196>

23. Palczewska, A., Palczewski, J., Robinson, R. M., & Neagu, D. (2013). Interpreting random forest classification models using a feature contribution method (extended). *2013 IEEE 14th International Conference on Information Reuse & Integration (IRI)*, 1–30. doi:10.1109/IRI.2013.6642461
24. Deng, H. (2019). Interpreting tree ensembles with inTrees. *International Journal of Data Science and Analytics*. doi:10.1007/s41060-018-0144-8
25. Strobl, C., Boulesteix, A. L., Kneib, T., Augustin, T., & Zeileis, A. (2008). Conditional variable importance for random forests. *BMC Bioinformatics*. doi:10.1186/1471-2105-9-307
26. Basu, S., Kumbier, K., Brown, J. B., & Yu, B. (2018). Iterative random forests to discover predictive and stable high-order interactions. *Proceedings of the National Academy of Sciences*. doi:10.1073/pnas.1711236115
27. Dessau, R. B., & Pipper, C. B. (2008). [’R’--project for statistical computing]. *Ugeskrift for læger*.
28. Carding, S., Verbeke, K., Vipond, D. T., Corfe, B. M., & Owen, L. J. (2015). Dysbiosis of the gut microbiota in disease. *Microbial Ecology in Health & Disease*. doi:10.3402/mehd.v26.26191
29. Levy, M., Kolodziejczyk, A. A., Thaiss, C. A., & Elinav, E. (2017). Dysbiosis and the immune system. *Nature Reviews Immunology*. doi:10.1038/nri.2017.7
30. Ai, D., Pan, H., Han, R., Li, X., Liu, G., & Xia, L. C. (2019). Using Decision Tree Aggregation with Random Forest Model to Identify Gut Microbes Associated with

- Colorectal Cancer. *Genes*, 10(2), 112. doi:10.3390/genes10020112
31. Vangay, P., Hillmann, B. M., & Knights, D. (2019). Microbiome learning Repo (ML Repo): A public repository of microbiome regression and classification tasks. *GigaScience*. doi:10.1093/gigascience/giz042
 32. Loh, G., & Blaut, M. (2012). Role of commensal gut bacteria in inflammatory bowel diseases. *Gut Microbes*. doi:10.4161/gmic.22156
 33. Nagao-Kitamoto, H., & Kamada, N. (2017). Host-microbial Cross-talk in Inflammatory Bowel Disease. *Immune Network*. doi:10.4110/in.2017.17.1.1
 34. Geirnaert, A., Calatayud, M., Grootaert, C., Laukens, D., Devriese, S., Smagghe, G., ... Van De Wiele, T. (2017). Butyrate-producing bacteria supplemented in vitro to Crohn's disease patient microbiota increased butyrate production and enhanced intestinal epithelial barrier integrity. *Scientific Reports*. doi:10.1038/s41598-017-11734-8
 35. Wang, Y., Gao, X., Ghoulane, A., Hu, H., Li, X., Xiao, Y., ... Zhang, T. (2018). Characteristics of faecal microbiota in paediatric Crohn's disease and their dynamic changes during infliximab therapy. *Journal of Crohn's and Colitis*. doi:10.1093/ecco-jcc/jjx153
 36. Wright, E. K., Kamm, M. A., Wagner, J., Teo, S. M., Cruz, P. De, Hamilton, A. L., ... Kirkwood, C. D. (2017). Microbial Factors Associated with Postoperative Crohn's Disease Recurrence. *Journal of Crohn's & colitis*. doi:10.1093/ecco-jcc/jjw136
 37. Y.-J., C., H., W., S.-D., W., N., L., Y.-T., W., H.-N., L., ... Shen, X.-Z. (2018).

Parasutterella, in association with irritable bowel syndrome and intestinal chronic inflammation. *Journal of Gastroenterology and Hepatology (Australia)*.

doi:10.1111/jgh.14281

38. Berry, D., Rahman, S., Kaplan, J., & Gordon, N. (2018). Probiotic and prebiotic compositions, and methods of use thereof for treatment and prevention of graft versus host disease. *USPTO*.
39. Yang, C., Fang, X., Zhan, G., Huang, N., Li, S., Bi, J., ... Hashimoto, K. (2019). Key role of gut microbiota in anhedonia-like phenotype in rodents with neuropathic pain. *Translational Psychiatry*. doi:10.1038/s41398-019-0379-8
40. Carpinelli, L., Bucci, C., Santonicola, A., Zingone, F., Ciacci, C., & Iovino, P. (2019). Anhedonia in irritable bowel syndrome and in inflammatory bowel diseases and its relationship with abdominal pain. *Neurogastroenterology and Motility*. doi:10.1111/nmo.13531
41. Rabizadeh, S., Rhee, K. J., Wu, S., Huso, D., Gan, C. M., Golub, J. E., ... Sears, C. L. (2007). Enterotoxigenic *Bacteroides fragilis*: A potential instigator of colitis. *Inflammatory Bowel Diseases*. doi:10.1002/ibd.20265
42. Wang, K., Yang, Q., Ma, Q., Wang, B., Wan, Z., Chen, M., & Wu, L. (2018). Protective effects of salvianolic acid a against dextran sodium sulfate-induced acute colitis in rats. *Nutrients*. doi:10.3390/nu10060791

